REVIEW

The year in cardiology 2016: imaging

Victoria Delgado[1], Oliver Gaemperli[2], Massimo Lombardi[3], Philipp A. Kaufmann[4], Jeroen J. Bax[1]*

Received: February 27, 2017. Accepted: February 28, 2017.

PREAMBLE

Cardiovascular diseases remain the main cause of death in Europe.[1] Current mortality statistics show that more than 4 million people die from cardiovascular diseases every year. Non-invasive cardiovascular imaging plays a central role in the diagnosis and management of patients with cardiovascular diseases. In 2016, many articles focused on prognostic impact of current non-invasive imaging techniques and technological innovations were published. A selection of these articles on the use of non-invasive cardiovascular imaging, including echocardiography, computed tomography (CT), cardiovascular magnetic resonance imaging (CMR), nuclear imaging, and fusion imaging is presented here.

ECHOCARDIOGRAPHY

Echocardiography is the imaging technique of first choice to evaluate patients with cardio-kardivascular diseases. A recent analysis of the largest, publicly available, all-payer inpatient database of the United States has shown that during 2001 and 2011 approximately 7 669 000 echocardiograms were performed and a steady increase in the volume of echocardiograms was noted with an average annual grew rate of 3.41%.[2] Although these numbers would suggest an overuse of this diagnostic procedure, the results from the 2010 nationwide inpatient sample showed otherwise. When analysing five clinical scenarios accounting for 3.7 million hospital admissions (cerebrovascular disease, cardiac arrhythmia, chronic heart failure, acute myocardial infarction, and sepsis), echocardiography was performed only in 8% of the cases indicating a significant underuse of echocardiography. Importantly, the use of echocardiography was associated with significantly lower odds of all-cause in-hospital mortality in these five clinical scenarios. Additional studies will be warranted to provide more information on the association between access to echocardiography and clinical outcomes.

Lung ultrasound is another application of echocardiography and is considered a first-line test to assess pulmonary congestion in patients with suspected acute heart failure.[3] The detection of B-lines (reflection of discrete air/fluid interfaces between collapsed, fluid-filled, and well-aerated alveoli) on the anterolateral chest scan indicates a progressive increase of extravascular lung water. The number of Blines can be summed to generate a semiquantitative score of the extravascular lung water content.[4] The incremental diagnostic and prognostic value of the use of lung ul-

[1] Heart Lung Centrum, Leiden University Medical Center, Leiden, The Netherlands
[2] Cardiac Imaging, University Heart Center, Zurich, Switzerland
[3] Multimodality Cardiac Imaging Section, IRCCS Policlinico San Donato, San Donato Milanese Milan, Italy
[4] Department of Nuclear Medicine, Cardiac Imaging, University Hospital Zurich, Zürich, Switzerland

Contact address:
Jeroen J Bax, Heart Lung Centrum, Leiden University Medical Center, Albinusdreef 2, 2300 RC, Leiden, The Netherlands. / Phone: +31 71 526 2020; Fax: +31 71 526 6809
E-mail: j.j.bax@lumc.nl

trasound was investigated in 195 heart failure patients with New York Heart Association (NYHA) class II–IV symptoms evaluated at the outpatient clinic.[5] Of the 185 patients with adequate lung ultrasound data, 59 (32%) had ≥3 B-lines while only 17 (9%) had crackles on auscultation. Patients with higher number of B-lines showed more severe heart failure symptoms and higher levels of NT-pro brain natriuretic peptide. In addition, patients with ≥3 B-lines had a four-fold higher risk of the primary endpoint (hospitalization for worsening of heart failure or all-cause mortality) at 6 months follow-up compared with patients without B-lines (adjusted hazard ratio [HR] 4.08; 95% confidence interval [CI] 1.95–8.54; P < 0.001). The use of lung ultrasound provided incremental prognostic value over auscultation as shown by an incremental discrimination improvement of 6.4% for the primary endpoint. These results are promising and indicate that the use of lung ultrasound may help in the risk stratification of heart failure patients. Standardization of the technique, adequate training to obtain and interpret the data and demonstration that lung ultrasoundguided therapy results in better outcome will help to implement this imaging technique in clinical practice.[6]

Although left ventricular (LV) ejection fraction (EF) is an important criterion in the decision making of patients with cardiovascular disease, LV global longitudinal strain (GLS) measured with two-dimensional speckle tracking echocardiography has shown to be more sensitive than LVEF to detect subclinical LV systolic dysfunction and has incremental value to predict outcomes.[7] In a population-based cohort of 791 white Europeans (52% women, 50.8 ± 15.5 years old), Kuznetsova and colleagues demonstrated the incremental prognostic value of LV GLS to predict the occurrence of cardiovascular events (i.e. coronary events, stroke, new-onset atrial fibrillation, heart failure, life-threatening arrhythmias, and aortic events).[8] During a median follow-up of 7.9 years (5729 person-years of follow-up), 96 individuals presented at least with one cardiovascular event (16.8 events per 1000 person-years). On multivariate analysis, each 1 SD decrease in LV GLS was associated with 75% increase in the risk of cardiovascular events. Furthermore, the addition of LV GLS to a model containing several demographic and clinical covariates resulted in a moderate improvement in the ability of the model to discriminate between patients with and without events (net reclassification improvement 0.31; P = 0.003). The incremental prognostic value of LV GLS over LVEF was additionally demonstrated in a study including 1065 heart failure patients with reduced LVEF.[9] The primary endpoint (all-cause mortality) was reached by 177 (16.7%) patients after a median follow-up of 40 months. Patients who died showed worse LVEF (23.8 ± 9.9% vs. 28.2 ± 9.1%; P < 0.001) and GLS (-8.1 ± 3.0% vs. -9.9 ± 3.2%, P < 0.001) compared with patients who were alive. When patients were divided according to GLS tertiles, patients within the highest GLS tertile group (most impaired GLS) had three times higher risk of all-cause mortality compared with patients of the lowest tertile (best GLS) (HR 3.38, 95% CI 2.3–5.1; P < 0.001). After adjusting for clinical and echocardiographic variables, LV GLS was the only echocardiographic parameter independently associated with all-cause mortality (HR 1.15 per each 1% increase – less negative – in GLS; P = 0.008) and its addition to the model resulted in 9.27% increment in the net reclassification improvement. These findings suggest that, even in patients with poor LVEF, LV GLS shows even more deteriorated LV performance and improves risk stratification. Assessment of LV systolic function may be more complicated in patients with reduced LVEF and significant secondary mitral regurgitation. By unloading the LV into the left atrium, LVEF may overestimate the true LV systolic function. The hypothesis that LV GLS may better reflect the true LV systolic function in patients with significant mitral regurgitation was tested in a study including 150 non-ischaemic cardiomyopathy patients, 50% of them with significant secondary mitral regurgitation.[10] Despite having comparable LVEF as per inclusion criteria, patients with significant mitral regurgitation had significantly more impaired LV GLS compared with patients without (-8.08 ± 3.33 vs. -9.78 ± 3.78%, respectively; P = 0.004) (Figure 1).

Three-dimensional transoesophageal echocardiography (TEE) data of the mitral valve analysed with proprietary software has shown important differences in mitral valve deformation (strain) along the systolic phase in patients with organic mitral regurgitation and normal controls:[11] the posterior mitral leaflet showed higher strain intensity than the anterior mitral leaflet and the distribution of high strain was consistently observed in the commissures, boundary zones near the mitral annulus and coaptation line while the central leaflet zone had the lowest strain. Although patients with organic mitral regurgitation had higher strain intensities in the anterior and posterior mitral leaflets compared with controls, the distribution of high strain was similar. The clinical implications of these findings

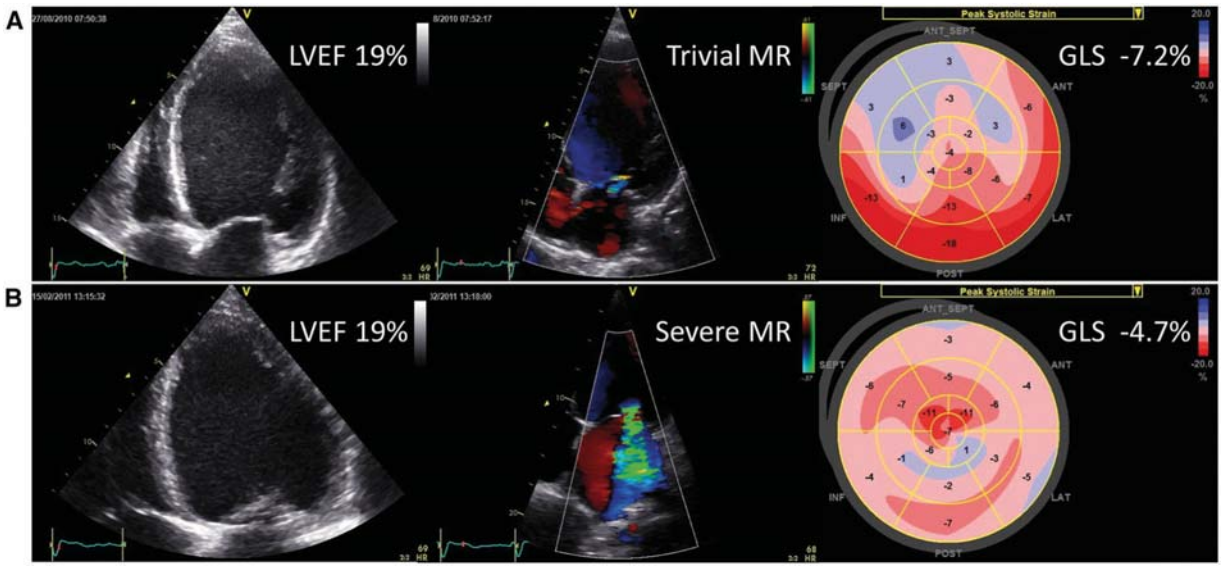

Figure 1. Left ventricular global longitudinal strain vs. left ventricular ejection fraction to assess left ventricular systolic function in patients with secondary mitral regurgitation. Example of two patients with non-ischaemic cardiomyopathy.
Despite comparable left ventricular ejection fraction (LVEF), the patient with severe mitral regurgitation (MR) has more impaired left ventricular global longitudinal strain (GLS) as compared with the patient without MR.
Reproduced with permission of Oxford University Press from Kamperidis et al.[10]
This figure has been reprinted by permission of Oxford University Press on behalf of the European Society of Cardiology.

need further investigations. Finally, it has been suggested that the aortic valve calcification burden may be associated with sex and aortic valve haemodynamics. In a large cohort of 888 patients with severe aortic stenosis who underwent aortic valve replacement, Thaden et al. showed that male sex, current smoking, bicuspid morphology, and larger LV outflow tract area were independently associated with high weight of the excised aortic valve whereas diabetes and hypertension were associated with lower weight of aortic valve.[12] Despite similar aortic valve area, male had higher aortic valve weight and calcification burden than women suggesting that the aortic valve stenosis severity does not explain sex-related differences in excised aortic valve weight and calcification burden.

COMPUTED TOMOGRAPHY

The year 2016 has witnessed a number of important publications in the field of cardiovascular CT. In 5185 participants of the Multi-Ethnic Study of Atherosclerosis (MESA), Yeboah et al. explored the incremental prognostic value of non-traditional risk markers (coronary artery calcium score [CACS], anklebrachial index, high-sensitivity C-reactive protein, and family history of atherosclerotic cardiovascular disease [ASCVD] over traditional risk estimation by the pooled cohort equation (the current standard of risk estimation recommended by the American College of Cardiology [ACC]/American Heart Association [AHA] guidelines).[13] Of all risk markers, CACS was the only parameter to improve the predictive accuracy of the pooled cohort equation as measured by a significant albeit modest increase in the Harrel's c-statistic (0.76 vs. 0.74, P = 0.04) and a total net reclassification improvement of 0.119 (95% CI, 0.080–0.256). Current ACC/AHA cholesterol management guidelines have broadened indications for statins in primary prevention raising concerns of overtreatment and increased costs.[14] In another MESA publication, Nasir and colleagues explored the value of a zero CACS to reclassify patients currently eligible for statins into a low-risk category where statin therapy may no longer be required.[15] Of 2966 participants eligible for statins (i.e. statin either recommended or considered), 1316 (44%) had a CACS = 0 at baseline and an observed 10-year ASCVD event rate of 4.2 per 1000 person-years. Thus, more widespread use of CACS may help to 'de-risk' a sizable number of subjects where statin therapy for primary prevention could be avoided.

In a substudy of the Prospective Multicenter Imaging Study for Evaluation of Chest Pain (PROMISE) trial, quality-of-life (QoL) outcomes of an anatomical (coronary CT angiography [CTA]) vs. functional diagnostic testing strategy were assessed in 5985 stable coronary artery disease (CAD) patients.[16] At 24 months, there were no strategy-related differences in

the Duke Activity Status Index and the Seattle Angina Questionnaire frequency scale, or any of the secondary QoL measures. The randomized Computed Tomography vs. Exercise Testing in Suspected Coronary Artery Disease (CRESCENT) trial had a similar design than PROMISE albeit with a considerably smaller study population (n = 350).17 Moreover, patients in the anatomical arm followed a tiered CT protocol including a 'gate-keeper' CACS scan followed by coronary CTA only if CACS was between 1 and 400. After 1.2 years, event-free survival was 96.7% for patients randomized to CT and 89.8% for patients randomized to functional testing (P = 0.011). After CT, the final diagnosis was established sooner, and additional downstream testing was required less frequently, resulting in lower cumulative diagnostic costs (€369 vs. €440; P < 0.0001). Taken together, PROMISE and CRESCENT further document non-inferiority of an initial CT-based anatomical imaging strategy compared with traditional functional testing strategies (i.e. stress ECG, stress echocardiography, myocardial perfusion scintigraphy) in stable CAD patients.

The Better Evaluation of Acute Chest Pain with Computed Tomography Angiography (BEACON) study randomized 500 low-risk patients with acute chest pain presenting to the emergency department of seven Dutch hospitals to immediate coronary CTA vs. standard care including serial testing with high-sensitivity troponin assays (hsTrop).[18] The coronary CTA group had lower direct medical costs (€337 vs. €511, P < 0.01) and less outpatient testing after the index emergency department visit (4% vs. 10%, P < 0.01). However, (in contrast to previously published American trials with standard troponin assays) there were no differences in the number of revascularizations, the emergency department discharge rates, or the length of stay. Hence, in the era of hsTrop (allowing more accurate and faster rule-out of myocardial infarction), the BEACON study questions the utility of early coronary CTA in suspected acute coronary syndrome patients.

CT-derived fractional flow reserve (FFR_{CT}) continues to raise interest in 2016: in a substudy of the Analysis of Coronary Blood Flow Using CT Angiography: Next Steps (NXT)-trial, Gaur and colleagues evaluated the association between coronary stenosis severity, plaque characteristics and FFR_{CT} in 484 vessels from 254 patients.[19] The presence of low-density non-calcified plaque (≥30 mm^3) and FFR_{CT} (≤0.80) increased significantly the diagnostic accuracy of coronary stenoses to detect lesion-specific ischemia (as assessed by invasive FFR), documented by an increase in the area under the receiver operating characteristic curve from 0.71 to 0.90 (P < 0.001). The non-randomized Prospective LongitudinAl Trial of FFR_{CT}: Outcome and Resource IMpacts (PLATFORM) trial assessed the impact of FFR_{CT} on clinical outcomes, downstream resource utilization and costs in two parallel observational arms, one with an intended invasive strategy (n = 380) and one with planned non-invasive testing (n = 204).[20] In the planned invasive stratum, FFR_{CT} lowered mean costs by 33% ($8,127 vs. $12,145; P < 0.0001) on 1 year follow-up; however, in the planned non-invasive stratum, mean costs were slightly higher when using an FFR_{CT} cost weight equal to coronary CTA.

Beyond coronary arteries, this year's CT publications have highlighted the clinical potential of the technique to assess valvular disease. Early hypo-attenuated leaflet thickening (HALT) of trans-catheter aortic valve implants (TAVI) has emerged as a new entity with uncertain prognostic and therapeutic implications. Pache and colleagues followed 156 TAVI patients with early routine coronary CTA (a median of 5 days post-TAVI with a balloon-expandable prosthesis) and found HALT in 16 (10.3%) patients (Figure 2).[21] The occurrence of HALT was not associated with antiplatelet regimen or any of the baseline or procedural characteristics. HALT did not produce any symptoms but

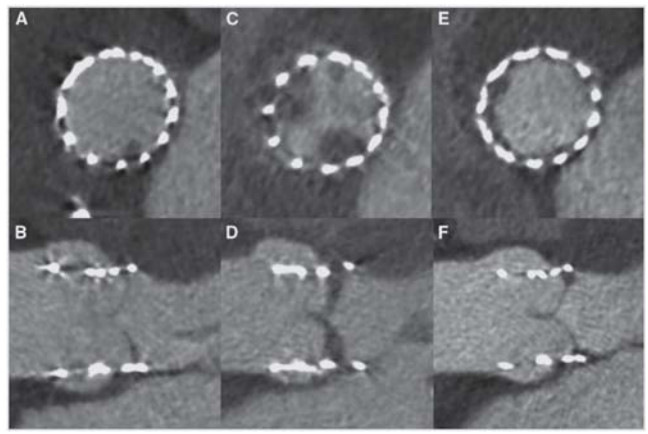

Figure 2. Axial and sagittal oblique reconstructions of a CORONARY CTA scan in an 80-year-old female immediately after implantation of a balloon-expandable transcatheter aortic valve prosthesis (A and B), at 3 months- (C and D), and at 6 months-follow-up (E and F). Note subtle early hypo-attenuated thickening (HALT) of the non-coronary cusp (A and B) which progressed to 5 mm thickening of the non-coronary cusp and included the right coronary cusp (C and D). After a combination of clopidogrel and phenprocoumon follow-up coronary CTA showed almost complete resolution of HALT. (E and F).
Reproduced with permission of Oxford University Press from Pache et al.[21]
This figure has been reprinted by permission of Oxford University Press on behalf of the European Society of Cardiology.

was associated with restrictive cusp motion and slightly higher transaortic mean pressure gradient (14.9 ± 5.3 vs. 11.6 ± 3.4 mmHg, P = 0.026). Full anticoagulation restored normal cusp morphology and motion in almost all patients. Gündüz and colleagues investigated the utility of CT to distinguish pannus from thrombus after surgical aortic valve replacement.[22] In 37 patients with mechanical prosthetic aortic valve dysfunction and evidence of periprosthetic mass, CT demonstrated significantly lower attenuation of thrombotic masses (defined as masses which completely resolved upon thrombolysis or were surgically identified as a clot) compared with pannus (87 ± 59 vs. 322 ± 122 Hounsfield units [HU]; P < 0.001). A cut-off at 145 HU provided high sensitivity (87.5%) and specificity (95.5%) in discriminating pannus from thrombus. Finally, CT has also demonstrated clinical value for the assessment of mitral paravalvular leakage after surgical mitral valve replacement. Suh and co-workers compared the diagnostic accuracy of CT, transthoracic echocardiography, and TEE in 204 patients with previous surgical mitral valve replacement, of which 78 underwent redo surgery.[23] CT had very comparable accuracy to TEE, but appeared to have superior sensitivity and negative predictive value than transthoracic echocardiography (although the difference did not reach statistical significance). TEE, however, was better in predicting the exact location of paravalvular leakage than CT (86% vs. 76%).

CARDIOVASCULAR MAGNETIC RESONANCE

The evidence showing the diagnostic and prognostic value of CMR techniques in individuals with increased cardiovascular risk, patients with valvular heart disease or patients with cardiomyopathies is accumulating. The underlying pathophysiological mechanisms of aortopathy in patients with bicuspid aortic valve have been the focus of extensive CMR research. To demonstrate how transvalvular rheological disturbances influence the expression and severity of aortopathy associated with aortic stenosis, Girdauskas et al.[24] evaluated with conventional CMR 190 patients with severe aortic stenosis who underwent surgical aortic valve replacement with or without concomitant surgery of the proximal ascending aorta: 137 patients had a bicuspid aortic valve while the remaining 53 had a tricuspid aortic valve. Aortopathy was defined by an end-diastolic cross-sectional diameter ≥22 mm/m^2 or ≥40 mm at any level of the proximal aorta. The proportion of patients with aortopathy was higher among patients with bicuspid aortic valve as compared to patients with tricuspid valve (35% vs. 11%, P = 0.008). In terms of CMRderived rheological parameters, patients with bicuspid aortic valve had greater angle between the LV outflow tract and the aortic root and more frequently asymmetric aortic valve orifice compared with their counterparts. On logistic regression analysis, only the angle between the LV outflow tract and the aortic root, and the angle between the systolic flow jet and the aortic wall were independently associated with aortopathy whereas valve morphology was not associated, suggesting that, in patients with aortic stenosis, these rheological variables may be more related to aortopathy than aortic valve morphology *per se*. Four-dimensional flow CMR has provided further insight into the relation between blood flow patterns in the ascending aorta and valve morphology.[25,26] Using this technique, Garcia et al.[25] showed in 50 patients with bicuspid and 50 patients with tricuspid aortic valve and dilated aorta that patients with bicuspid aortic valve have higher peak flow jet velocity between the LV outflow tract and the sinotubular junction compared with patients with tricuspid valve, despite having comparable aortic dimensions. On multivariate analysis, age and peak flow jet velocity were the only significant correlates of maximal aortic dimensions. Furthermore, in 37 patients with various grades of aortic stenosis and 37 healthy volunteers, helical and vertical flow formations and flow eccentricity were assessed in the ascending aorta using four-dimesional flow CMR.[26] Compared with healthy volunteers, patients with aortic stenosis showed more frequently marked helical and vertical flow formation and eccentric flow with asymmetrical and elevated distribution of peak systolic wall stress in the ascending aorta. Smaller aortic orifice areas were associated with more vertical flow formation and eccentric flow and higher flow displacement whereas bicuspid aortic valve morphology was significantly associated with intense helical flow formation and higher flow displacement and peak systolic wall shear stress.

Tissue characterization with late gadolinium enhancement (LGE) and T1 mapping CMR techniques have shown to be more sensitive than electrocardiographic parameters or biomarkers to detect myocardial scar and fibrosis. Of 1840 participants in the MESA study who were free of clinical cardiovascular disease at baseline (in 2000–2002) and underwent LGE CMR in the 10th year examination (2010–2012), 146 (7.9%) indivi-

duals showed myocardial scar.[27] In 78% of them, myocardial scar was unrecognized by electrocardiogram or clinical evaluation. Age, male sex, body mass index, hypertension, and CACS (adjusted for age, sex, and ethnicity) at baseline were associated with presence of myocardial scar at year 10. The odds ratio for myocardial scar of a CACS value ≥400 was three-fold higher compared with CACS of 0. The prognostic implications of these findings were not evaluated. The association between presence of midwall myocardial scar/fibrosis and adverse outcomes in patients with aortic stenosis was investigated by Chin et al.[28] From 147 patients with mild-to-severe aortic stenosis and no prior myocardial infarction who underwent LGE CMR, a score including clinical, biomarker, echocardiographic, and electrocardiographic variables independently associated with the presence of midwall myocardial scar/fibrosis was derived. Low risk of myocardial fibrosis was defined by a risk score of <7% whereas high risk was defined by a risk score of >57%. The prognostic value of this score was validated in two cohorts of asymptomatic patients with at least mild aortic stenosis: 127 patients from an internal cohort and 289 patients from an external cohort, resulting in 1560 patient-years. In the internal cohort, a high risk score was associated with seven-fold higher mortality rates compared with patients with low risk score (13 vs. 2.1 all-cause death/100 patient-years; P < 0.001). Similarly, in the external cohort, high-risk patients had 31.6 aortic stenosis related events (cardiovascular death, heart failure and new symptoms)/100 patient-years compared with 4.6 aortic stenosis related events/100 patient-years in the low-risk patients (P < 0.001).

Assessment of reactive diffuse myocardial fibrosis with T1 mapping techniques has permitted differentiation between hypertrophic cardiomyopathy and LV hypertrophy secondary to hypertension.[29] Native T1 times and extracellular volume fraction (ECV) reflect the amount of interstitial myocardial fibrosis. The International T1 Multicenter CMR study included 95 patients with hypertrophic cardiomyopathy, 69 patients with essential hypertension, 23 carriers of sarcomere gene mutations without LV hypertrophy and 23 healthy volunteers. Patients with hypertrophic cardiomyopathy had longer native T1 times (1169 ± 41 ms vs. 1058 ± 29 ms, P < 0.001) and higher ECV (0.31 ± 0.06 vs. 0.24 ± 0.04, P < 0.001) compared with hypertensive patients. Interestingly, sarcomere gene mutation carriers had significantly longer native T1 times as compared with healthy volunteers (1105 ± 17 ms vs. 1044 ± 18 ms, P < 0.001) but similar ECV. Therefore, T1-mapping CMR techniques permit as well early detection of structural changes in mutation carriers who have not developed yet the phenotype. Similarly, differentiation between patients with early non-ischaemic dilated cardiomyopathy and individuals with physiological adaptation to exercise ('athlete's heart') has been possible with calculation of native T1 times, ECV and T2 times.[30] Patients with early presentation of dilated cardiomyopathy displayed significantly larger native T1 times, ECV and T2 times (indicating replacement fibrosis) as compared with individuals performing aerobic exercise more than 6 h per week (Figure 3). These techniques have also helped to better understand the LV diastolic function of patients with heart failure and preserved LVEF. In 24 patients with heart failure and preserved LVEF, Rommel et al.[31] showed that ECV was an independent predictor of invasively measured LV stiffness constant (r = 0.75; P < 0.01). Furthermore, patients with an ECV below the median (32.3%) were characterized by prolonged active LV relaxation whereas patients with an ECV above the median showed higher LV stiffness constant suggesting differences in the pathological mechanisms of symptoms. In the field of myocarditis, the MyoRacer-Trial assessed the diagnostic accuracy of T1 and T2 mapping CMR techniques in 129 patients with suspected myocarditis (61 with acute and 68 with chronic symptoms).[32] Biventricular endomyocardial biopsy was performed in 93% of patients. In the group with acute symptoms, native T1 mapping yielded the higher area under the curve to diagnose myocarditis (0.82, P = 0.002) followed by T2 mapping (0.81, P = 0.001) and ECV (0.75, P = 0.04) as compared with Lake Louise criteria (0.56). In patients with chronic symptoms, T2 mapping permitted differentiation between myocarditis and no myocarditis patients and provided a significantly higher area under the curve (0.77) compared with native T1 mapping (0.53, P = 0.004) and Lake Loiuse criteria (0.53, P = 0.002). Finally, the prognostic implications of T1 mapping CMR techniques were evaluated in a prospective multicentre study which included 637 consecutive patients with non-ischaemic cardiomyopathy.[33] D uring a median follow-up of 22 months, 28 patients died (22 from cardiac cause) and 68 composite heart failure events were recorded. Each 10 ms increase in native T1 time was independently associated with 10% increase in the risk of all-cause mortality and 7% increase in the risk of composite heart failure events.

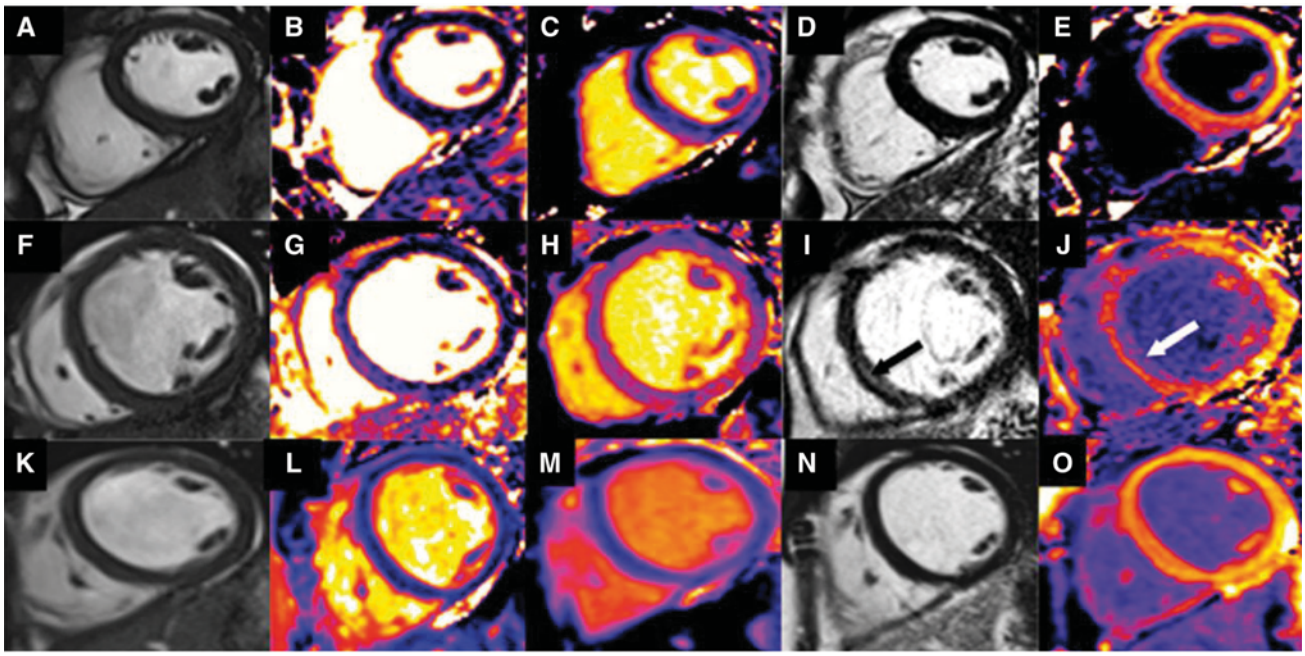

Figure 3. Native T1 time, extracellular volume and T2 time assessed with CMR to differentiate between the early phase of dilated cardiomyopathy and an 'athlete's heart'. CMR data acquisition in a healthy control (panels A–E), a patient with dilated cardiomyopathy (panels F–J) and an individual with 'athlete's heart' (panels K–O). The healthy control had normal LVEF (58%, panel A), the septal T2 time was 51.6 ms (panel B), the septal native T1 time was 924.9 ms (panel C) and there was no LGE (panel D) or diffuse fibrosis (ECV 27%, panel E). In contrast, the patient with dilated cardiomyopathy showed mildly reduced LVEF (48%, panel F), septal T2 time 59.8 ms (panel G), septal native T1 time 1017.8 ms (panel H) and midwall fibrosis in the inferoseptum (panel I, arrow) on LGE and significant diffuse fibrosis as reflected by an ECV of 35% (panel J, arrow). In the individual with 'athlete's heart', the LVEF was relatively preserved (53%, panel K), the septal T2 time was 50.4 ms (panel L), the native T1 time was 931.4 ms (panel M) and there was no LGE (panel N) and the value of ECV was similar to that of the healthy individual (28%, panel O). Accordingly, early stages of dilated cardiomyopathy show mildly reduced function and development of replacement fibrosis, phenomena not observed in healthy individuals or patients with 'athlete's heart'.
Reproduced with permission from Mordi et al.[30]
This Figure has been reprinted by permission of Oxford University Press on behalf of the European Society of Cardiology.

The efficacy of new transcatheter therapies for mitral regurgitation such as the MitraClip device (Abbott Vascular, Menlo Park, CA) is defined by reduction in mitral regurgitation grade, reverse remodelling of cardiac chambers and improvement in LVEF and symptoms. Cardiovascular magnetic resonance imaging is considered the reference standard to assess cardiac chamber volumes. In 20 patients undergoing MitraClip implantation, LV and right ventricular volumes and function (including feature tracking circumferential and radial strain) were assessed at baseline and 7 days after the procedure.[34] Although there was a significant improvement in heart failure symptoms and reduction in mitral regurgitation, there was neither significant reverse remodelling nor improvement in systolic function of the LV and right ventricle. Probably, CMR was performed too early after the procedure to observe any meaningful change in ventricular volumes and function. However, the device does not affect the image quality to assess ventricular volumes.

NUCLEAR IMAGING

Various articles were dedicated to improved detection of CAD. Lee et al.[35] performed 13N-ammonia positron emission tomography (PET) and derived quantitative measures such as hyperaemic myocardial blood flow, coronary flow reserve, and relative flow reserve for comparison with invasive FFR (<0.8) which is considered the reference for detecting functionally significant coronary artery stenoses. This study provides optimal cut-off values for 13N-ammonia PET for the diagnosis of significant CAD, being 1.99 mL/min/g for hyperaemic myocardial blood flow, 2.12 for coronary flow reserve and 0.82 for relative flow reserve. While all quantitative PET measures performed significantly better than relative perfusion defect assessment, relative flow reserve showed the highest diagnostic accuracy to predict the functional significance of a stenosis.

In the Clinical Evaluation of Magnetic Resonance Imaging in Coronary Heart Disease-2 (CE-MARC 2) multicenter randomized clinical trial, Greenwood et

al.[36] assessed whether non-invasive imaging-guided care is superior to National Institute for Health and Care Excellence (NICE) guidelinesdirected care in reducing unnecessary angiography (primary endpoint), defined as no significant coronary artery stenosis based on FFR measurement >0.8 or <70% stenosis on quantitative coronary angiography. A total of 1202 symptomatic patients with suspected CAD were enrolled and randomized to stress CMR, myocardial perfusion scintigraphy (MPS) or NICE guidelines-directed care. Within 12 months of follow-up, the endpoint occurred in 69 (28.8%) patients in the NICE guidelines-directed care group, which was significantly reduced to 36 (7.5%) in the CMR group and to 34 (7.1%) in the MPS group (P < 0.001 for both vs. NICE, with MPS and CMR being not significantly different).

The role of nuclear imaging in heart failure was highlighted by sub-analyses of two important prospective trials: the PET and Recovery Following Revascularization (PARR-2) study and the Adreview Myocardial Imaging for Risk Evaluation in Heart Failure (ADMIRE-HF).[37-39] The PARR-2 study is the karlargest randomized trial evaluating the prognostic benefit of 18F-fluorodeoxyglucose (FDG) PET-assisted management vs. standard care in patients with severe LV dysfunction and CAD considered for revascularization or transplantation; the 5-year outcome data revealed no differences in the composite event rate (cardiac death, infarction, or cardiac hospitalization): 53% in the PET arm vs. 57% in the standard care arm (HR 0.82, 95% CI 0.62–1.07; P = 0.15).[39] However, if only patients who adhered to the recommendation of the FDG PET scan were included, the outcome was significantly improved in PET-assisted management (HR 0.73, 95% CI 0.54–0.99; P = 0.042). The results suggest that evaluation of myocardial viability with PET can aid in the decision making of patients with ischaemic LV dysfunction who are considered for revascularization.

The ADMIRE-HF study demonstrated that assessment of myocardial sympathetic innervation with 123I-meta-iodobenzylguanidine (mIBG) scintigraphy has incremental prognostic information in heart failure patients and may identify patients with increased risk of ventricular arrhythmias or sudden cardiac death.[40] In a sub-study of the ADMIRE-HF trial, Hachamovitch et al.[38] investigated whether the use of ^{123}I-mIBG imaging to guide implantable cardioverter defibrillator (ICD) implantation will result in improved patient prognosis and efficiency of care. Of 777 patients (65% ischaemic heart disease) who did not have an ICD at the time of the index ^{123}I-mIBG scan, 75 (9.6%) died, 23 (3%) presented with sudden cardiac death and 26 (3.3%) with life-threatening arrhythmias during a median of 17 months. Planar ^{123}I-mIBG imaging was an independent and incremental predictor of all-cause mortality. In addition, in the extension study of the ADMIRE-HF trial (ADMIRE-HFX), the prognostic significance of patterns of ^{123}I-mIBG uptake (reflecting myocardial denervation) and ^{99}mTc-tetrofosmin myocardial perfusion imaging was assessed in 619 ischaemic and 319 non-ischaemic heart failure patients.[37] The extent and severity of myocardial denervation were quantified as percentage of total myocardium and the segment denervation score was calculated based on a 17-segment model using a 5-point scale. Moreover, the area of mismatch between ^{123}I-mIBG/^{99}mTc-tetrofosmin uptake was calculated. Mortality was higher in patients with denervation involving >50% of the myocardium. The highest cardiac mortality risk for ischaemic heart failure patients was observed with perfusion defects involving 20–40% of the myocardium. In contrast, non-ischaemic heart failure patients with smaller perfusion abnormalities (<20% of myocardium), but with a large discrepancy between ^{123}I-mIBG and ^{99}mTc-tetrofosmin defect sizes, were at highest risk of cardiac death, suggesting a potential prognostic role of the degree of denervation in areas with preserved myocardial perfusion in non-ischaemic heart failure patients.

An excessive catecholamine stimulation of the myocardium has been proposed as potential underlying mechanism of Tako-tsubo cardiomyopathy, a reversible cause of heart failure. To test this hypothesis, Christensen et al.[41] evaluated at admission and follow-up the sympathetic cardiac innervation with ^{123}I-mIBG scintigraphy and plasma cathecolamine levels in 32 patients diagnosed with Tako-tsubo cardiomyopathy and 20 controls. At admission, Tako-tsubo cardiomyopathy patients showed lower cardiac ^{123}I-mIBG uptake and higher levels of epinephrine compared with controls. At follow-up, cardiac ^{123}I-mIBG uptake normalized whereas the plasma epinephrine levels remained elevated in the Tako-tsubo cardiomyopathy patients. This hyperadrenergic activity may play a central role in the pathogenesis of this cardiomyopathy and may have important implications for clinical management.

Finally, nuclear imaging techniques have provided important diagnostic information in patients with suspected endocarditis. Caobelli et al.[42] performed dual-isotope imaging in 34 patients with suspected endocarditis of native (n = 12) or prosthetic (n = 22) valves

employing ^{111}In-labeled white blood cells (WBC) and ^{99}mTc for perfusion imaging on a dedicated cadmium-zinc-telluride (CZT) detector equipped SPECT (Figure 4). The high-energy resolution and sensitivity of novel CZT detector equipped camera enable simultaneous imaging of multiple isotopes enhancing the detection of molecular/cellular signals. Compared with standard ^{111}In-WBC planar scintigraphy and SPECT, dual-isotope CZT imaging yielded superior image quality, improved reader confidence, and improved diagnostic accuracy based on surgery or Duke Criteria during follow-up, thus demonstrating feasibility and added diagnostic value.

HYBRID IMAGING

It is clear that hybrid imaging (integrating two imaging modalities, mostly PET-CMR or PET-CT) is claiming a position in cardiovascular evaluations. Sometimes it is not necessary to use hybrid imaging equipment, but simple fusion of the separate images is also feasible. For example, fusion of coronary CTA and SPECT images has been performed previously, but the image fusion and presentation has been further developed by Nakahara et al.:[43] with this approach it is possible to present the SPECT bull's eye plot overlaid with the coronary arteries. In addition, Maffessanti and colleagues developed fusion software that combines three-dimensional displays of the coronary anatomy obtained with coronary CTA with colour maps of LV longitudinal strain obtained with threedimensional echocardiography, permitting visualization of the coronary stenosis along with its functional consequences (reduced LV strain) (Figure 5).[44]

Specifically in the field of molecular imaging, hybrid imaging becomes increasingly used to understand pathophysiology in CAD, with specific focus on vulnerable plaque imaging. Bala and colleagues used PET-CT and fluorine-18 labelled vascular cell adhesion molecule (VCAM)-1 (anti-VCAM-1 nanobody, cAbVCAM-1–5), to demonstrate the feasibility in a murine-atherosclerotic model to detect aortic plaque inflammation.[45] Increased tracer uptake was detected in aortic regions with increased atherosclerosis both on PET-CT and on histology. This is just one of the many studies ongoing to obtain further insight in differences between vulnerable and stable atherosclerotic plaques. In the short-term, more animal studies are needed focusing on the coronary arteries, then translational studies to patients, and finally outcome studies.

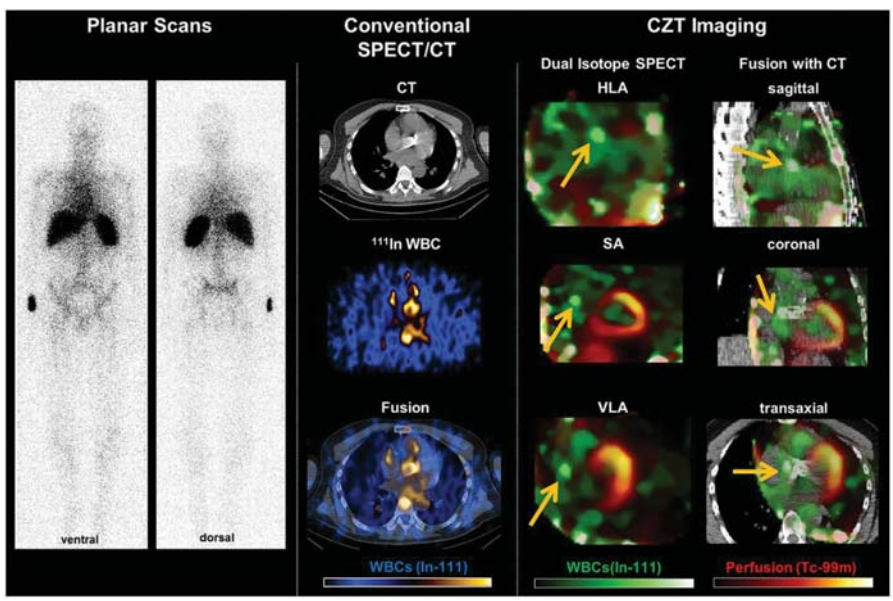

Figure 4. Evaluation of prosthetic valve endocarditis with nuclear imaging techniques. Representative images of a patient with suspected endocarditis of aortic valve prosthesis. From left to right, planar white blood cell scans show blood pool, with uncertainty about a valvular focus, whereas conventional SPECT/CT images suggest a potential hot spot in the region of the prosthetic valve, but with limited resolution. Dual isotope cadmium-zinc-telluride (CZT) images show reduced noise and a focal accumulation adjacent to the prosthetic valve suggesting the presence of endocarditis (arrows). During surgical aortic valve replacement, an abscess was identified under the right coronary artery ostium, matching the hot spot on the CZT scan and confirming the diagnosis of endocarditis.
HLA = horizontal long-axis; In = Indio; SA = short-axis; VLA= vertical long-axis; WBC = white blood cells.
Reproduced with permission from Caobelli et al.[42]
This Figure has been reprinted by permission of Oxford University Press on behalf of the European Society of Cardiology.

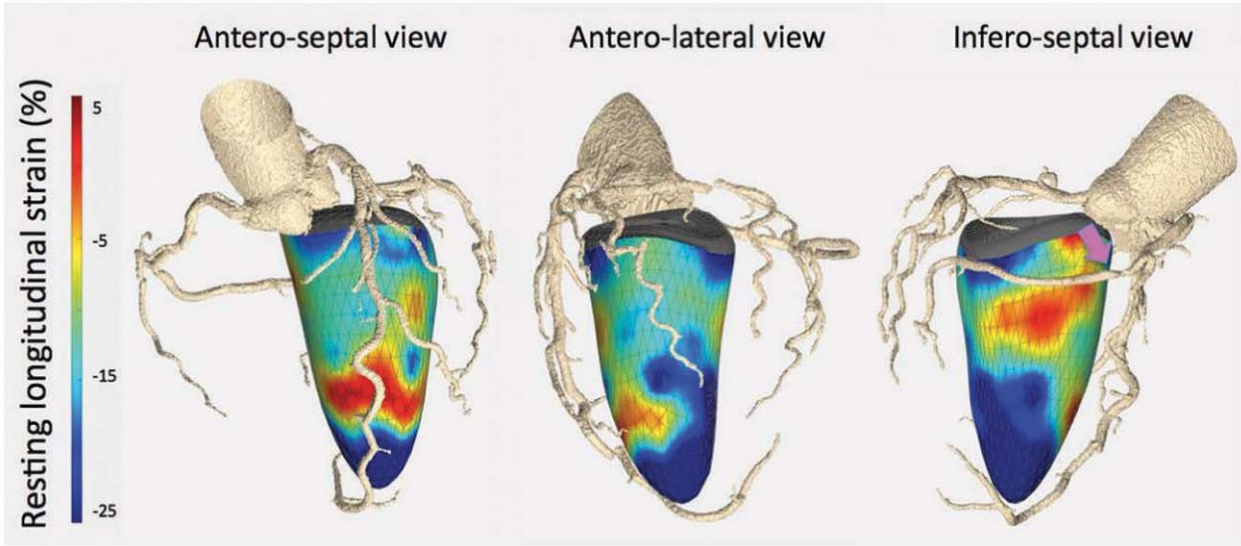

Figure 5. Fusion imaging of coronary CTA and three-dimensional speckle tracking echocardiography to assess the functional consequences of coronary stenosis. Combined three-dimensional displays of speckle tracking and CTA, in a patient with >70% stenosis in the mid right coronary artery (purple arrow). The infero-septal view shows reduced LV longitudinal strain in the basal segment (colour-coded in orange shades) subtended by this coronary artery. In addition, note a diffuse calcified plaque in the proximal left anterior descending coronary artery present causing reduced LV longitudinal strain in the mid-apical segments of the antero-septal view.
Reproduced with permission from Maffessanti et al.[44]
This Figure has been reprinted by permission of Oxford University Press on behalf of the European Society of Cardiology.

Positron emission tomography-cardiovascular magnetic resonance imaging (PET-CMR) is another modality that is increasingly used, and already some clinical studies in patients have been reported this year. Bulluck and coworkers used PET-CMR and FDG in 21 patients with ST-segment–elevation myocardial infarction (STEMI) 5 days after infarction, and follow-up scans were obtained 1 year later in 12 patients.[46] Cardiovascular magnetic resonance imaging was used to assess the infarct size (using late contrast-enhanced CMR) and the area at risk (using T2-mapping). Immediately after infarction, the area of reduced FDG uptake was significantly larger than the infarct size on late contrast-enhanced CMR (37.2 ± 11.6% vs. 22.3 ± 11.7%; P < 0.001), but was similar to the area at risk on CMR T2-mapping (37.2 ± 11.6% vs. 36.3 ± 12.2%; P = NS). On the 1-year follow-up scans, the area of reduced FDG uptake was significantly smaller as compared with the acute scans (19.5 [6.3–31.8%] vs. 44.0 [21.3–55.3%]; P = 0.002) and correlated closely with the area of infarction on late contrast-enhanced CMR. These findings contribute to our understanding of scar formation over time after acute myocardial infarction.

Rischpler et al.[47] used PET-CMR from a different perspective, namely to explore the value of FDG uptake in the infarct area (defined by late contrast-enhanced CMR) as a biosignal to predict functional recovery. In 49 patients, PET-CMR was performed within 5 days after infarction, and follow-up CMR (to assess functional recovery) was performed 6–9 months later. Comparison of PET-CMR with circulating leucocytes and monocytes was performed to measure cellular innate immune response. Fluorodeoxyglucose uptake in the infarcted area exceeded late gadolinium enhancement extent (33.2 ± 16.2% LV myocardium vs. 20.4 ± 10.6%, P < 0.0001) and corresponded to the area at risk (r = 0.87, P < 0.0001), indicating that FDG uptake early after infarction may be a biosignal of myocardial injury. The peripheral blood count of CD14high/CD16+ monocytes correlated with the infarction size and FDG uptake, supporting the hypothesis that FDG uptake reflects injury. Moreover, the FDG uptake in the infarcted myocardium was highest in areas with transmural scar, and was related inversely with functional recovery. All these findings may change our view on FDG uptake early after infarction, namely that it represents myocardial injury rather than viability.

Conflict of interest: The Department of Cardiology of the Leiden University Medical Center received research grants from Biotronik, Boston Scientific, Edwards Lifesciences and Medtronic. Victoria Delgado received speaker fees from Abbott Vascular, outside the submitted work. Oliver Gaemperli reports per-

sonal fees from Servier, non-financial support from Amgen, outside the submitted work. Massimo Lombardi has nothing to disclose. Jeroen Bax has nothing to disclose.

Drug and material disclaimer: The mention of trade names, commercial products organizations, and the inclusion of advertisements in the journal does not imply endorsement by the European Heart Journal, the editors, the editorial board, Oxford University Press or the organization to which the authors are affiliated. The editors and publishers have taken all reasonable precautions to verify drug names and doses, the results of experimental work and clinical findings published in the journal. The ultimate responsibility for the use and dosage of drugs mentioned in the journal and in interpretation of published material lies with the medical practitioner, and the editors and publisher cannot accept liability for damages arising from any error or omissions in the journal. Please inform the editors of any errors. The opinions expressed in the European Heart Journal are those of the authors and contributors, and do not necessarily reflect those of the European Society of Cardiology, the editors, the editorial board, Oxford University Press or the organization to which the authors are affiliated.

OUP and the ESC are not responsible or in any way liable for the accuracy of the translation, for any errors, omissions or inaccuracies, or for any consequences arising therefore. Dora Fabijanović and Saša Pavasović are solely responsible for the translation published in this reprint. Translation edited by: Mario Ivanuša. Language editing: Tomislav Salopek.

References

1. Townsend N, Wilson L, Bhatnagar P, Wickramasinghe K, Rayner M, Nichols M. Cardiovascular disease in Europe: epidemiological update 2016. Eur Heart J. 2016;37:3232-3245. https://doi.org/10.1093/eurheartj/ehw334
2. Papolos A, Narula J, Bavishi C, Chaudhry FA, Sengupta PP. U.S. hospital use of echocardiography: insights from the nationwide inpatient sample. J Am Coll Cardiol. 2016;67:502-511. https://doi.org/10.1016/j.jacc.2015.10.090
3. Lancellotti P, Price S, Edvardsen T, Cosyns B, Neskovic AN, Dulgheru R, et al. The use of echocardiography in acute cardiovascular care: recommendations of the European Association of Cardiovascular Imaging and the Acute Cardiovascular Care Association. Eur Heart J Cardiovasc Imaging. 2015;16:119-146. https://doi.org/10.1093/ehjci/jeu210
4. Picano E, Pellikka PA. Ultrasound of extravascular lung water: a new standard for pulmonary congestion. Eur Heart J. 2016;37:2097-2104. https://doi.org/10.1093/eurheartj/ehw164
5. Platz E, Lewis EF, Uno H, Peck J, Pivetta E, Merz AA, et al. Detection and prognostic value of pulmonary congestion by lung ultrasound in ambulatory heart failure patients. Eur Heart J. 2016;37:1244-1251. https://doi.org/10.1093/eurheartj/ehv745
6. Aras MA, Teerlink JR. Lung ultrasound: a 'B-line' to the prediction of decompensated heart failure. Eur Heart J. 2016;37:1252-1254. https://doi.org/10.1093/eurheartj/ehw094
7. Smiseth OA, Torp H, Opdahl A, Haugaa KH, Urheim S. Myocardial strain imaging: how useful is it in clinical decision making? Eur Heart J. 2016;37:1196-1207. https://doi.org/10.1093/eurheartj/ehv529
8. Kuznetsova T, Cauwenberghs N, Knez J, Yang WY, Herbots L, D'hooge J, et al. Additive prognostic value of left ventricular systolic dysfunction in a population-based cohort. Circ Cardiovasc Imaging. 2016;9:e004661. https://doi.org/10.1161/CIRCIMAGING.116.004661
9. Sengel øv M, Jørgensen PG, Jensen JS, Bruun NE, Olsen FJ, Fritz-Hansen T, et al. Global longitudinal strain is a superior predictor of all-cause mortality in heart failure with reduced ejection fraction. JACC Cardiovasc Imaging. 2015;8:1351-1359. https://doi.org/10.1016/j.jcmg.2015.07.013
10. Kamperidis V, Marsan NA, Delgado V, Bax JJ. Left ventricular systolic function assessment in secondary mitral regurgitation: left ventricular ejection fraction vs. speckle tracking global longitudinal strain. Eur Heart J. 2016;37:811-816. https://doi.org/10.1093/eurheartj/ehv680
11. Ben Zekry S, Freeman J, Jajoo A, He J, Little SH, Lawrie GM, et al. Patient-specific quantitation of mitral valve strain by computer analysis of threedimensional echocardiography: a Pilot Study. Circ Cardiovasc Imaging2016;9:e003254. https://doi.org/10.1161/CIRCIMAGING.115.003254
12. Thaden JJ, Nkomo VT, Suri RM, Maleszewski JJ, Soderberg DJ, Clavel MA, et al. Sex-related differences in calcific aortic stenosis: correlating clinical and echocardiographic characteristics and computed tomography aortic valve calcium score to excised aortic valve weight. Eur Heart J. 2016;37:693-699. https://doi.org/10.1093/eurheartj/ehv560
13. Yeboah J, Young R, McClelland RL, Delaney JC, Polonsky TS, Dawood FZ, et al. Utility of nontraditional risk markers in atherosclerotic cardiovascular disease risk assessment. J Am Coll Cardiol. 2016 January19;67:139-147. https://doi.org/10.1016/j.jacc.2015.10.058
14. Stone NJ, Robinson JG, Lichtenstein AH, Bairey Merz CN, Blum CB, Eckel RH, et al; American College of Cardiology/American Heart Association Task Force on Practice Guidelines. 2013 ACC/AHA guideline on the treatment of blood cholesterol to reduce atherosclerotic cardiovascular risk in adults: a report of the American College of Cardiology/American Heart Association Task Force on Practice Guidelines. Circulation. 2014 Jun 24;129(25 Suppl 2):S1-45. https://doi.org/10.1161/01.cir.0000437738.63853.7a
15. Nasir K, Bittencourt MS, Blaha MJ, Blankstein R, Agatson AS, Rivera JJ, et al. Implications of coronary artery calcium testing among statin candidates according to American College Of Cardiology/American Heart Association cholesterol management guidelines: MESA (Multi-Ethnic Study of Atherosclerosis). J Am Coll Cardiol. 2015;66:1657-1668. https://doi.org/10.1016/j.jacc.2015.07.066
16. Mark DB, Anstrom KJ, Sheng S, Baloch KN, Daniels MR, Hoffmann U, et al. Quality-of-life outcomes with anatomic versus functional diagnostic testing strategies in symptomatic patients with suspected coronary artery disease: results from the PROMISE randomized trial. Circulation. 2016;133:1995-2007. https://doi.org/10.1161/CIRCULATIONAHA.115.020259
17. Lubbers M, Dedic A, Coenen A, Galema T, Akkerhuis J, Bruning T, et al. Calcium imaging and selective computed tomography angiography in comparison to functional testing for suspected coronary artery disease: the multicentre, randomized CRESCENT trial. Eur Heart J. 2016;37:1232-1243. https://doi.org/10.1093/eurheartj/ehv700
18. Dedic A, Lubbers MM, Schaap J, Lammers J, Lamfers EJ, Rensing BJ, et al. Coronary CT angiography for suspected ACS in the era of high-sensitivity troponins: randomized multicenter study. J Am Coll Cardiol. 2016;67:16-26. https://doi.org/10.1016/j.jacc.2015.10.045
19. Gaur S, Øvrehus KA, Dey D, Leipsic J, Bøtker HE, Jensen JM, et al. Coronary plaque quantification and fractional flow reserve by coronary computed tomography angiography identify ischaemia-causing lesions. Eur Heart J. 2016;37:1220-1227. https://doi.org/10.1093/eurheartj/ehv690
20. Douglas PS, De BB, Pontone G, Patel MR, Norgaard BL, Byrne RA, et al. 1-year outcomes of FFRct-guided care in patients with sus-

pected coronary disease: the PLATFORM study. J Am Coll Cardiol. 2016;68:435-445. https://doi.org/10.1016/j.jacc.2016.05.057
21. Pache G, Schoechlin S, Blanke P, Dorfs S, Jander N, Arepalli CD, et al. Early hypo-attenuated leaflet thickening in balloon-expandable transcatheter aortic heart valves. Eur Heart J. 2016;37:2263-2271. https://doi.org/10.1093/eurheartj/ehv526
22. Gündüz S, Ozkan M, Kalcik M, Gursoy OM, Astarcioglu MA, Karakoyun S, et al. Sixty-four-section cardiac computed tomography in mechanical prosthetic heart valve dysfunction: thrombus or pannus. Circ Cardiovasc Imaging. 2015;8:e003246. https://doi.org/10.1161/CIRCIMAGING.115.003246
23. Suh YJ, Hong GR, Han K, Im DJ, Chang S, Hong YJ, et al. Assessment of mitral paravalvular leakage after mitral valve replacement using cardiac computed tomography: comparison with surgical findings. Circ Cardiovasc Imaging. 2016;9:e004153. https://doi.org/10.1161/CIRCIMAGING.115.004153
24. Girdauskas E, Rouman M, Disha K, Fey B, Dubslaff G, Theis B, et al. Functional aortic root parameters and expression of aortopathy in bicuspid versus tricuspid aortic valve stenosis. J Am Coll Cardiol. 2016;67:1786-1796. https://doi.org/10.1016/j.jacc.2016.02.015
25. Garcia J, Barker AJ, Murphy I, Jarvis K, Schnell S, Collins JD, et al. Four-dimensional flow magnetic resonance imaging-based characterization of aortic morphometry and haemodynamics: impact of age, aortic diameter, and valve morphology. Eur Heart J Cardiovasc Imaging. 2016;17:877-884. https://doi.org/10.1093/ehjci/jev228
26. von Knobelsdorff-Brenkenhoff F, Karunaharamoorthy A, Trauzeddel RF, Barker AJ, Blaszczyk E, Markl M, et al. Evaluation of aortic blood flow and wall shear stress in aortic stenosis and its association with left ventricular remodeling. Circ Cardiovasc Imaging. 2016;9:e004038. https://doi.org/10.1161/CIRCIMAGING.115.004038
27. Turkbey EB, Nacif MS, Guo M, McClelland RL, Teixeira PB, Bild DE, et al. Prevalence and correlates of myocardial scar in a US cohort. JAMA. 2015;314:1945-1954. https://doi.org/10.1001/jama.2015.14849
28. Chin CW, Messika-Zeitoun D, Shah AS, Lefevre G, Bailleul S, Yeung EN, et al. A clinical risk score of myocardial fibrosis predicts adverse outcomes in aortic stenosis. Eur Heart J. 2016;37:713-723. https://doi.org/10.1093/eurheartj/ehv525
29. Hinojar R, Varma N, Child N, Goodman B, Jabbour A, Yu CY, et al. T1 Mapping in Discrimination of Hypertrophic Phenotypes: Hypertensive Heart Disease and Hypertrophic Cardiomyopathy: Findings From the International T1 Multicenter Cardiovascular Magnetic Resonance Study. Circ Cardiovasc Imaging. 2015;8:e003285. https://doi.org/10.1161/CIRCIMAGING.115.003285
30. Mordi I, Carrick D, Bezerra H, Tzemos NT. T1 and T2 mapping for early diagnosis of dilated non-ischaemic cardiomyopathy in middle-aged patients and differentiation from normal physiological adaptation. Eur Heart J Cardiovasc Imaging. 2016;17:797-803. https://doi.org/10.1093/ehjci/jev216
31. Rommel KP, von Roeder M, Latuscynski K, Oberueck C, Blazek S, Fengler K, et al. Extracellular volume fraction for characterization of patients with heart failure and preserved ejection fraction. J Am Coll Cardiol. 2016;67:1815-1825. https://doi.org/10.1016/j.jacc.2016.02.018
32. Lurz P, Luecke C, Eitel I, Fohrenbach F, Frank C, Grothoff M, et al. Comprehensive cardiac magnetic resonance imaging in patients with suspected myocarditis: the MyoRacer-Trial. J Am Coll Cardiol. 2016;67:1800-1811. https://doi.org/10.1016/j.jacc.2016.02.013
33. Puntmann VO, Carr-White G, Jabbour A, Yu CY, Gebker R, Kelle S, et al. T1-Mapping and outcome in nonischemic cardiomyopathy: all-cause mortality and heart failure. JACC Cardiovasc Imaging. 2016;9:40-50. https://doi.org/10.1016/j.jcmg.2015.12.001
34. Lurz P, Serpytis R, Blazek S, Seeburger J, Mangner N, Noack T, et al. Assessment of acute changes in ventricular volumes, function, and strain after interventional edge-to-edge repair of mitral regurgitation using cardiac magnetic resonance imaging. Eur Heart J Cardiovasc Imaging. 2015;16:1399-1404. https://doi.org/10.1093/ehjci/jev115
35. Lee JM, Kim CH, Koo BK, Hwang D, Park J, Zhang J, et al. Integrated myocardial perfusion imaging diagnostics improve detection of functionally significant coronary artery stenosis by 13N-ammonia positron emission tomography. Circ Cardiovasc Imaging. 2016;9:e004768. https://doi.org/10.1161/CIRCIMAGING.116.004768
36. Greenwood JP, Ripley DP, Berry C, McCann GP, Plein S, Bucciarelli-Ducci C, et al; CE-MARC 2 Investigators. Effect of care guided by cardiovascular magnetic resonance, myocardial perfusion scintigraphy, or NICE guidelines on subsequent unnecessary angiography rates: The CE-MARC 2 randomized clinical trial. JAMA. 2016;316:1051-1060. https://doi.org/10.1001/jama.2016.12680
37. Clements IP, Kelkar AA, Garcia EV, Butler J, Chen J, Folks R, et al. Prognostic significance of (123)I-mIBG SPECT myocardial imaging in heart failure: differences between patients with ischaemic and non-ischaemic heart failure. Eur Heart J Cardiovasc Imaging. 2016;17:384-390. https://doi.org/10.1093/ehjci/jev295
38. Hachamovitch R, Nutter B, Menon V, Cerqueira MD. Predicting risk versus predicting potential survival benefit using 123I-mIBG imaging in patients with systolic dysfunction eligible for implantable cardiac defibrillator implantation: analysis of data from the prospective ADMIRE-HF study. Circ Cardiovasc Imaging. 2015;8:e003110. https://doi.org/10.1161/CIRCIMAGING.114.003110
39. Mc Ardle B, Shukla T, Nichol G, deKemp RA, Bernick J, Guo A, et al; PARR-2 Investigators. Long-term follow-up of outcomes with F-18-fluorodeoxyglucose positron emission tomography imaging-assisted management of patients with severe left ventricular dysfunction secondary to coronary disease. Circ Cardiovasc Imaging. 2016;9:e004331. https://doi.org/10.1161/CIRCIMAGING.115.004331
40. Jacobson AF, Senior R, Cerqueira MD, Wong ND, Thomas GS, Lopez VA, et al; ADMIRE-HF Investigators. Myocardial iodine-123 meta-iodobenzylguanidine imaging and cardiac events in heart failure. Results of the prospective ADMIRE-HF (AdreView Myocardial Imaging for Risk Evaluation in Heart Failure) study. J Am Coll Cardiol. 2010;55:2212-2221. https://doi.org/10.1016/j.jacc.2010.01.014
41. Christensen TE, Bang LE, Holmvang L, Skovgaard DC, Oturai DB, Soholm H, et al. (123)IMIBG scintigraphy in the subacute state of Takotsubo cardiomyopathy. JACC Cardiovasc Imaging. 2016;9:982-990. https://doi.org/10.1016/j.jcmg.2016.01.028
42. Caobelli F, Wollenweber T, Bavendiek U, Kuhn C, Schutze C, Geworski L, et al. Simultaneous dual-isotope solid-state detector SPECT for improved tracking of white blood cells in suspected endocarditis. Eur Heart J. 2017;38:436-443. https://doi.org/10.1093/eurheartj/ehw231
43. Nakahara T, Iwabuchi Y, Murakami K. Diagnostic performance of 3D bull's eye display of SPECT and coronary CTA fusion. JACC Cardiovasc Imaging. 2016;9:703-711. https://doi.org/10.1016/j.jcmg.2015.09.024
44. Maffessanti F, Patel AR, Patel MB, Walter JJ, Mediratta A, Medvedofsky D, et al. Non-invasive assessment of the haemodynamic significance of coronary stenosis using fusion of cardiac computed tomography and 3D echocardiography. Eur Heart J Cardiovasc Imaging. 2017 Jun 1;18(6):670-680. https://doi.org/10.1093/ehjci/jew147
45. Bala G, Blykers A, Xavier C, Descamps B, Broisat A, Ghezzi C, et al. Targeting of vascular cell adhesion molecule-1 by 18F-labelled nanobodies for PET/CT imaging of inflamed atherosclerotic plaques. Eur Heart J Cardiovasc Imaging. 2016;17:1001-1008. https://doi.org/10.1093/ehjci/jev346
46. Bulluck H, White SK, Frohlich GM, Casson SG, O'meara C, Newton A, et al. Quantifying the area at risk in reperfused ST-segment-elevation myocardial infarction patients using hybrid cardiac positron emission tomography-magnetic resonance imaging. Circ Cardiovasc Imaging. 2016;9:e003900. https://doi.org/10.1161/CIRCIMAGING.115.003900
47. Rischpler C, Dirschinger RJ, Nekolla SG, Kossmann H, Nicolosi S, Hanus F, et al. Prospective evaluation of 18F-Fluorodeoxyglucose uptake in postischemic myocardium by simultaneous positron emission tomography/magnetic resonance imaging as a prognostic marker of functional outcome. Circ Cardiovasc Imaging. 2016;9:e004316. https://doi.org/10.1161/CIRCIMAGING.115.004316.